Turkish Journal of Chemistry

http://journals.tubitak.gov.tr/chem/

Research Article

Turk J Chem
(2015) 39

doi:10.3906/kim-1401-56

Kinetics and performance studies of a switchable solvent TMG (1,1,3,3-tetramethylguanidine)/1-propanol/carbon dioxide system

Özge YÜKSEL ORHAN[1,*], Mustafa Çağdaş ÖZTÜRK[2], Ayça ŞEKER[1], Erdoğan ALPER[1]

[1]Department of Chemical Engineering, Faculty of Engineering, Hacettepe University, Ankara, Turkey
[2]Department of Chemical and Biological Engineering, Armour College of Engineering, Illinois Institute of Technology, Chicago, IL, USA.

Received: 20.01.2014 • **Accepted:** 09.05.2014 • **Published Online:** 23.01.2015 • **Printed:** 20.02.2015

Abstract: The rate constants and the activation energies of the reaction between carbon dioxide and 1,1,3,3-tetramethylguanidine (TMG) in 1-propanol solution were measured by a stopped-flow technique at a temperature range of 288–308 K and at a TMG concentration range of 2.5–10.0 wt %. Based on the pseudo-first-order reaction for CO_2, the reaction was modeled by a termolecular reaction mechanism, which resulted in a rate constant of 199.30 m^3 $kmol^{-1}$ s^{-1} at 298 K. The activation energies were 5.19 kJ/mol and 5.26 kJ/mol at 2.5 and 5.0 wt % TMG, respectively. In addition, carbon dioxide absorption capacity was investigated using a gas–liquid contact system. Absorption capacity of the 10.0 wt % TMG/1-propanol system was found to be 0.035 mol CO_2/0.035 mol TMG, indicating a favorable loading ratio of 1:1. Repeatability and potential performance losses of this system were analyzed by Fourier transform infrared spectrometry (FTIR) in the range of 400–4000 cm^{-1}. It was found that the FTIR spectra of the rich solvent became virtually identical to the spectra of the lean solvent upon thermal desorption, promising efficient regeneration. It is therefore concluded that the TMG/1-propanol/CO_2 system is easily switchable and can be used both for carbon dioxide capture and for other applications that require rapid change of medium from nonionic to ionic liquid.

Key words: Binding organic liquids, carbon capture, reaction kinetics, reaction mechanism, stopped-flow method, switchable solvents, 1,1,3,3-tetramethylguanidine

1. Introduction

Carbon dioxide is produced at very high levels at thermal power plants and in different process industries, such as refining and petrochemicals, and cement and iron/steel plants. It is discharged into the atmosphere even though the emissions are desired to be limited according to the Kyoto Protocol. In order to store carbon dioxide safely (CO_2 sequestration) or to produce C1 chemicals from it, it is necessary to separate it from other nonacidic gases. Therefore, development of new solvents and CO_2 capture technologies has gained importance. The generally accepted method that is used today is to absorb carbon dioxide from gas mixtures into aqueous amine solutions with a reversible reaction. However, for these systems, the CO_2 loading ratio is limited to a maximum of 0.5 mol CO_2/mol amine and the regeneration of solvent by desorption takes place at 393–403 K.[1,2] Consequently, the energy requirements of the desorber (especially, the reboiler duty) become very high, leading to a rather costly process. Furthermore, subsequent corrosion to instruments has escalated the demand for alternative CO_2 capture systems. Therefore, there are ongoing efforts to design new solvents to increase the

*Correspondence: oyuksel@hacettepe.edu.tr

CO_2 loading capacity, as well as to reduce (or eliminate) the latent heat requirement of the aqueous systems, which come with the high specific heat of water (4187 J/(g K)). For instance, it is possible to increase the CO_2 loading ratio to a theoretical value of 1 by employing sterically hindered amines, whose carbamate ion is unstable.[3] Although the steric hindrance results in lower reaction rates, highly reactive activators such as piperazine and its derivatives can be used to increase the reaction rates.[4] In this respect, new blends of aqueous amines have also been developed.[5,6] By this method, it is possible to reduce the energy costs partially. However, since the reboiler is still required for desorption, the energy requirement could not be reduced significantly.

A potential solvent system for CO_2 capture is the CO_2-binding organic liquids (CO_2BOLs), which were developed in recent years.[7–10] CO_2BOLs are novel solvents comprising amidine or guanidine bases in an alcohol mixture (binary system) or alcohol functionalized strong amidine or guanidine base (single system).[11] The main advantages of these systems are high CO_2 loading capacities, low heat capacities, and low energy requirement during regeneration as compared to aqueous alkanolamine solutions[1,12,13]

Amidine and guanidine primary bases can be used for CO_2 capture due to their strong basic properties.[14–16] While a carbamate ion is formed by the reaction of primary and secondary amines with CO_2, amidinium or guanidinium alkyl carbonate salts occur with the reaction of CO_2BOLs and carbon dioxide.[9,17–19] It is thought that alkyl carbonate salts formed from CO_2BOLs do not form as many hydrogen bonds as carbamate and bicarbonate salts do. Therefore, the binding enthalpy of CO_2 decreases and high stripping temperatures that amine systems need are no longer required.[1,20]

It is known that when appropriate alcohol and base pairs (CO_2BOLs) react with CO_2 an ionic liquid is formed that causes a notable increase in polarity.[12,20] Moreover, CO_2BOLs can be regenerated below the boiling point of the mixture. In many cases, CO_2 is removed from the solution by simple heating or sweeping with an inert gas such as nitrogen. Then the solvent reverts to its nonionic form and is ready for future CO_2 uptake.[21] This class of reversible liquids, originally developed for other purposes, is also known as switchable solvents.[2,16,20,22–24] The most common switchable ionic liquids are composed of a mixture of 1,8-diazabicycloundec-7-ene (DBU) or 1,1,3,3-tetramethylguanidine (TMG) with an alcohol.[12,25,26] Regeneration of the solvent from ionic liquids can be carried out at lower temperatures than those used for amine solvents. At these regeneration temperatures (usually below 373 K), recovery of the solvent may be achieved with the use of a simple heat exchanger, rather than a reboiler.[12,27,28]

CO_2BOLs have high gravimetric and volumetric capacity in terms of carbon dioxide binding.[29] The first CO_2BOL (DBU/1-hexanol) was designed in 2005 and captures about 1.3 moles CO_2 per 1 mole of DBU at 1 atm, yielding a capture 19% by weight and 147 gCO_2/L liquid.[23] There are recent studies on CO_2 loading capacity and reaction kinetics of CO_2BOLs with carbon dioxide. One of these studies focused on the solvent system formed by 1,8-diazabicyclo[5.4.0]undec-7-ene base in 1-hexanol and 1-propanol.[30] However, the kinetics and the loading performance of the TMG/1-propanol/carbon dioxide system have not been studied before and therefore the aim of this work was to provide such data.

2. Theoretical

2.1. Reaction mechanism

Generally, CO_2-amine system reaction kinetics can be explained by 2 widely known mechanisms. These are the zwitterion and the termolecular reaction mechanisms. The following equations outline the possible reactions based on these 2 mechanisms.

The zwitterion mechanism, which was originally proposed by Caplow in 1968, and then reintroduced by Danckwerts in 1979, has been widely used to describe amine carbon dioxide kinetics and its validity was confirmed with further evidence.[31,32] This mechanism consists of 2 steps. The first step is the formation of a 2-charged structure by the reaction between carbon dioxide and the amine, which is called a zwitterion. In the next step, an amine-proton is transferred to a second molecule; the base-catalyzed deprotonation of the zwitterion takes place to produce carbamate ion and a protonated base. This reaction mechanism is generally used to describe the reaction kinetics of primary and secondary amines.[33]

For example, zwitterion formation for a primary amine is as follows:

$$CO_2 + RNH_2 \underset{k_{-1}}{\overset{k_2}{\rightleftharpoons}} RN^+H_2COO^- \tag{1}$$

This zwitterion loses a proton to a base, resulting in carbamate formation:

$$RN^+H_2COO^- + B \xrightarrow{k_B} RNHCOO^- + BH^+ \tag{2}$$

In this reaction, an amine, hydroxyl ions, water, or an alcohol can act as the base. In the step where the zwitterion is losing a proton, if the base is an amine, then the reaction is second order in amine.[34] The resulting net reaction is given in Eq. (3).

$$CO_2 + 2RNH_2 \rightleftharpoons RNHCOO^- + RNH_3^+ \tag{3}$$

Another applicable reaction mechanism is the termolecular or 3-molecular reaction mechanism. The basic principle of the termolecular reaction mechanism (also known as the single step mechanism), which was originally proposed by Crooks and Donellan and then revisited by Alper and da Silva and Svendsen, is the assumption that an amine reacts with both a carbon dioxide and a base molecule in a single step.[35–37] It is assumed that the reaction takes place via the weakly bound intermediate product as shown in Eq. (4).

$$CO_2 + RNH_2 \cdots B \rightleftharpoons RNHCOO^- \cdots BH^+ \tag{4}$$

As reported earlier, the termolecular mechanism can be adapted to CO_2BOL systems containing an amidine/guanidine and a linear alcohol.[30]

$$CO_2 + TMG + ROH \rightleftharpoons [TMGH^+][ROCOO^-] \tag{5}$$

Under pseudo-first-order (excess solvent) conditions, the observed forward reaction rate can be expressed as in Eq. (6).

$$r_{obs} = k_o[CO_2] \tag{6}$$

In the TMG/1-propanol system, alcohol may act as the proton carrier and also improve physical absorption. The system preserves its liquid form before and after the absorption of CO_2. Rate constants of TMG/1-propanol system components can be expressed by Eq. (7).

$$k_o = \{k_{TMG}[TMG] + k_{ROH}[ROH]\}[TMG] \tag{7}$$

Here, ROH concentration is assumed constant under excess ROH conditions and therefore a new rate constant, k, can be defined.

$$k = k_{ROH}[ROH] \tag{8}$$

$$k_o = \{k_{TMG}[TMG] + k\}[TMG] \tag{9}$$

Thus, reaction degree can change between 1 and 2 depending on the rate of the reaction. Furthermore, if the system exhibits a first-order reaction, Eq. (9) simplifies to the following equation:

$$k_o = k[TMG] \tag{10}$$

Both reaction mechanisms give rise to similar expressions for reaction kinetics under the abovementioned conditions. The zwitterion mechanism becomes equivalent to the termolecular mechanism when the lifetime of the zwitterion intermediate approaches zero.[37] Therefore, we prefer to use the termolecular reaction mechanism for our analysis.

3. Results and discussion

3.1. Absorption/desorption performance of TMG/1-propanol system

CO_2 absorption tests of 10 wt % TMG/1-propanol solution (0.035 mol TMG) using a 50-mL solution were performed at 303 K and at 2 bar. In order to investigate the regeneration efficiency of the CO_2-rich TMG/1-propanol solution, it was subjected to desorption under 343 K and 1.1 bar absolute pressure. The solution was exposed to 5 capture and release cycles. The capacities of the solution, the initial absorption rate, and time to reach the equilibrium are given in Table 1 for 5 absorption cycles.

Table 1. Cyclic absorption capacities, initial absorption rates, and equilibrium times for the 10 wt % TMG/1-propanol system at 303 K and 2 bar.

10 wt % TMG/1-propanol	Absorption capacity for CO_2 (mol)	Initial absorption rate (kmol/m^2 s) $\times$ (10^5)	Equilibrium time (min)
Absorption #1	0.035	3.42	35
Absorption #2	0.033	2.98	36
Absorption #3	0.034	2.84	37
Absorption #4	0.033	2.84	37
Absorption #5	0.032	2.69	36

It was found that the solution could be recycled 5 times without any considerable loss of capture capacity. The moles of carbon dioxide absorbed plotted against time shown in Figure 1.

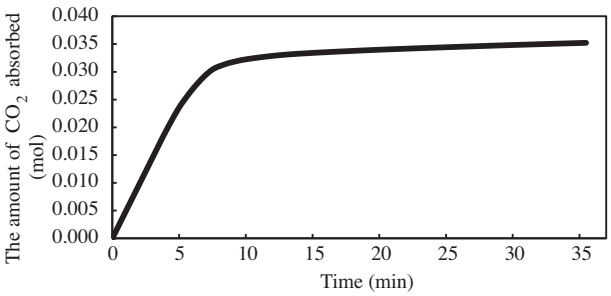

Figure 1. CO_2 loading graph (1st Absorption) of 10 wt % TMG/1-propanol system at 303 K.

As seen in Figure 1, the CO_2 uptake was completed within 35 min. The system reached equilibrium in a relatively short time, as a result of the solution being saturated with carbon dioxide and subsequent reduction in the driving force for mass transfer. Thus, the rate of absorption approaches zero. From Figure 1, for the 10.0 wt % TMG/1-propanol system, the capacity of the solution for the first absorption was calculated as 0.035 mol CO_2. This finding confirms that TMG/1-propanol is capable of chemically capturing 1 mol CO_2/mol TMG at 303 K in contrast to 0.5 mol CO_2/mol amine for MEA.

3.2. Fourier infrared transform spectroscopy (FTIR) analysis

FTIR analyses were also carried out to investigate the reversibility of reactions of carbon dioxide with TMG/1-propanol solution, as well as absorption/desorption performance losses. For this purpose, FTIR analysis of lean and rich CO_2BOL solutions was conducted with a Thermo Scientific NICOLET6700 model FTIR device.

First, the solvent was loaded to the equilibrium level with CO_2. Then CO_2-rich solvent was stripped by exposure to heat treatment in a nitrogen environment within the gas–liquid contact reactor, and FTIR analysis was repeated. As seen in Figure 2, fingerprint peaks of the characteristic C=O bond of loaded-CO_2 solution were observed at a wavelength of 1600–1700 cm^{-1}. After desorption, the C=O bond fingerprint peaks almost disappeared and a spectrum similar to that of the lean solvent was obtained. All of these procedures were repeated for the second absorption and desorption cycles and the reversibility of the reaction was seen to be maintained.

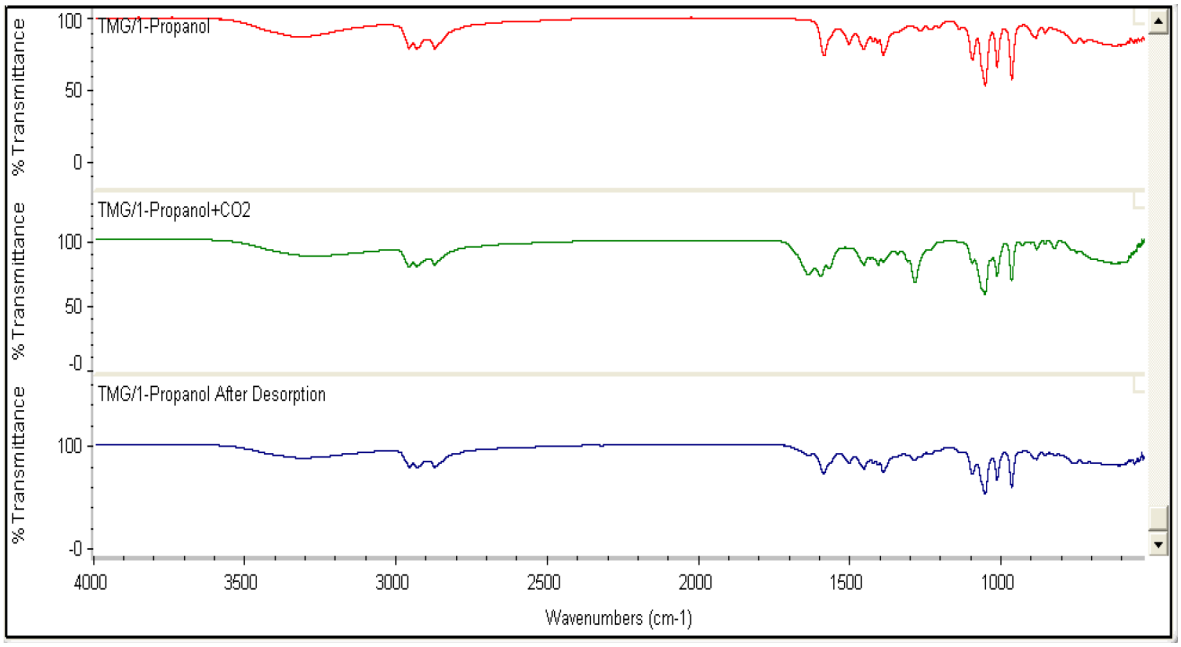

Figure 2. Fourier infrared transform spectroscopy (FTIR) analysis of TMG/1-propanol system.

3.3. Reaction rate constants

Table 2 summarizes the results for observed pseudo-first-order reaction rate constants (k_o) values versus the wt % concentration of the TMG/1-propanol system at temperatures ranging from 288 K to 308 K. The natural logarithms of reaction rate constants versus TMG concentrations were plotted to determine the empirical reaction order, as shown in Figure 3. Using the least squares method, empirical power law kinetics was fitted

to the line in Figure 3. Here, the slope corresponds to the reaction order of the TMG/1-propanol system, which is determined to be 0.992 ($\sim$1) with a regression value of $R^2 = 0.973$ for the concentration range of 0.350–1.430 kmol/m^3 at 298 K. This result is in agreement with a single-step termolecular reaction mechanism between the solvent and carbon dioxide in 1-propanol medium as given by Eq. (10). Therefore, the observed k_o values that were obtained experimentally were correlated using the termolecular mechanism to determine the forward reaction rate constant k [m^3 kmol^{-1} s^{-1}]. The reaction rate constants versus TMG concentration were plotted according to Eq. (6), with a satisfactory pseudo-first-order line fit, as seen in Figure 4. From the slope of the fitted line in Figure 4, the first-order forward reaction rate constant for the TMG/1-propanol system was determined to be 199.3 m^3 kmol^{-1} s^{-1}. The reaction rate and reaction order data as obtained for TMG/1-propanol are presented in Table 3.

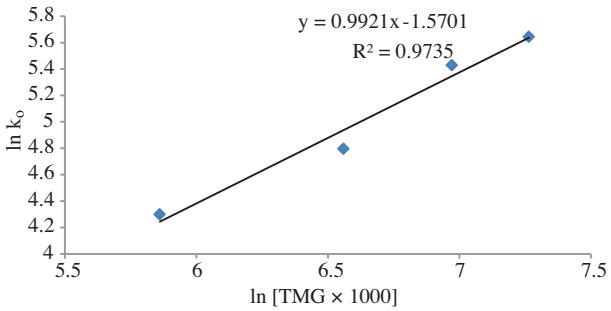

Figure 3. Empirical power law plots for the TMG/1-propanol system at 298 K.

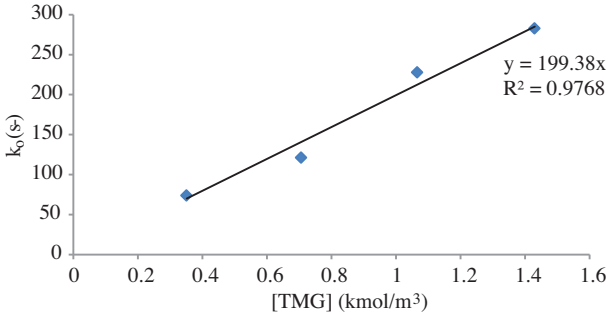

Figure 4. Changes in pseudo-first-order rate constants with increasing TMG concentration for the TMG/1-propanol system at 298 K.

Table 2. Observed k_o values for the TMG/1-propanol/CO_2 system at various temperatures and in different TMG concentrations.

	k_o, s^{-1}			
[TMG] (wt %)	2.5	5.0	7.5	10
288 K	66.78	113.50	-	-
293 K	72.78	121.72	-	-
298 K	73.65	121.02	227.67	282.68
303 K	75.18	125.50	-	-
308 K	76.77	128.38	-	-

Table 3. Summary of obtained kinetics data for the TMG/1-propanol system at 298 K.

k [m^3 kmol^{-1} s^{-1}]	k_{TMG} [m^6 kmol^{-2} s^{-1}]	Reaction order
199.30	-	0.992

Furthermore, to determine the activation energies, experiments were conducted at 2 concentrations and 5 temperatures, as shown in Table 2. The Arrhenius diagram was plotted as shown in Figure 5 and activation energies for both solvent systems were also calculated by evaluating the Arrhenius equation (Eq. (11)).

$$k = A\exp\left(-\frac{E_a}{RT}\right) \tag{11}$$

From Figure 5, activation energies for the TMG/1-propanol system were calculated as 5.19 kJ/mol at 2.5 wt % TMG and 5.26 kJ/mol at 5.0 wt % TMG.

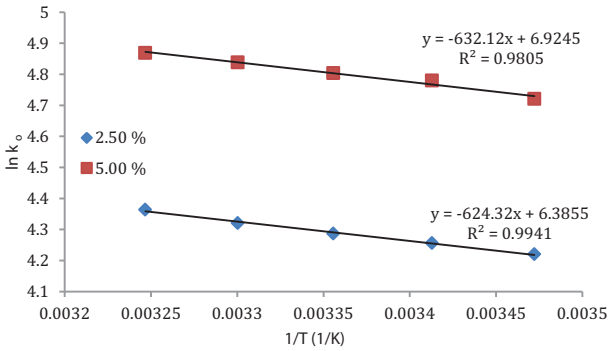

Figure 5. Arrhenius diagram for the TMG/1-propanol system.

Finally, the results obtained in this work were compared with the published data of other CO_2BOLs as shown in Table 4.

Table 4. Comparison of kinetics properties of various CO_2BOLs.

Amines	TMG/1-propanol	TMG/1-hexanol	DBU/1-propanol	DBU/1-hexanol
Reference	This work	Ozturk et al., 2014[40]	Ozturk et al., 2012a	Ozturk et al., 2012a
Reaction order, n at 298 K	0.99	0.98	1.24	1.21
k [m^3 $kmol^{-1}$ s^{-1}] at 298 K	199.30	64.1	677.9	626.9
E_A (kJ/mol)	5.23	9.76	15.61	13.67

4. Experimental

In this work, we use a stopped-flow conductimetry technique to analyze the reaction kinetics, a method particularly developed for fast homogeneous liquid reactions. Intrinsic reaction rates were measured with this technique. In addition, gas absorption experiments were carried out in a bench-scale gas–liquid contact reactor that operates semicontinuously and batchwise in terms of liquid. A mass flow controller controls the outgoing gas flow and the pressure, while the entering CO_2 gas is measured by a mass flow meter. Then the CO_2 absorption rate can be calculated by the balance of these measurements. The equipment can also be arranged to study the desorption kinetics.

4.1. Materials and methods

4.1.1. Reagents

TMG: 1,1,3,3-tetramethylguanidine (reagent-grade, CAS no. 80-70-6) with 99% purity was supplied by Sigma-Aldrich (St. Louis, MO, USA) and 1-propanol (CAS no. 71-23-8) with 99% purity was provided by J.T. Baker. Carbon dioxide gas was supplied by Linde (Germany) with 99.99% purity. These reagents were used without further purification. The experiments were carried out at 4 different concentrations of TMG (2.5, 5.0, 7.5, and 10.0 wt %) and at 5 different temperatures (288 K, 293 K, 298 K, 303 K, and 308 K).

4.1.2. Gas–liquid contact reactor

The absorption experiments were performed in a gas–liquid contact reactor (model RD-CSTR 200) capable of absorption analysis by measuring the volumetric flow rates of incoming and outgoing gas streams. The system operates at a temperature range of 293–363 K and a pressure range of 0–10 bar. It consists of a stainless steel reactor with a jacket, power control units for heating and stirring, mass flow meter (MFM) with a rating range of 1–100 cm^3/min, a mass flow controller (MFC), and a data acquisition system. The stainless steel tank jacket contains digital sensors connected to the data system, which provides temperature control of ± 0.5 K precision. The stirrer unit contains a stainless steel agitator, and a driver motor capable of a 50–500 rpm stirring rate. The schematic setup of the apparatus is shown in Figure 6.

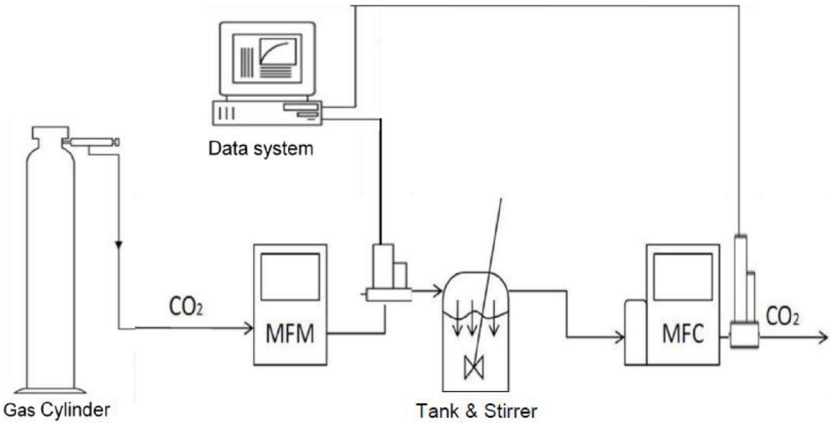

Figure 6. Systematic set-up of gas–liquid contact reactor, RD-CSTR 200.

During a run, pure CO_2 from a gas cylinder passes through a MFM to the reactor and the flow rate is recorded as a function of time. Then the gas stream reaches the reactor, where CO_2 contacts with the solvent (CO_2BOL) and the reaction takes place at a stirring speed of 500 rpm. Excess unabsorbed CO_2 leaves the reactor through a MFC at its predetermined value. As time passes, the solution becomes saturated with CO_2 and therefore the inlet flow rate of CO_2 to the reactor decreases, since the tank operates at constant pressure. The readings of the MFM and MFC, reactor pressure and temperature, measured by digital sensors, are recorded by the data acquisition system at 10-s intervals. The rate of CO_2 absorption by the CO_2BOLs can be inferred from the difference between MFM and MFC readings for a specific time interval. The experiment is terminated when the MFM values approach the set MFC values. The time evolution of CO_2 absorption is analyzed by plotting a graph of MFM readings (cm^3/min) versus the reaction time. Each of the areas shown in Figure 7 represents the amount of CO_2 absorbed during 10-s time intervals. The total amount of CO_2 absorbed by the solution can be calculated by summing those areas. Then the moles of CO_2 absorbed by a specific concentration of TMG solution were calculated by converting the balance of MFM and MFC readings (cm^3/min) into moles of CO_2. This numerical integration method allows the calculation of the amount of loaded CO_2 at any desired time during the experiments.[38]

The change in CO_2 loading against time enables the determination of the solution capacity and initial absorption rate. A typical example of a CO_2 loading chart is shown in Figure 8.

From Figure 8, the amount of CO_2 captured by the TMG solution was determined until the system approaches equilibrium. Furthermore, the absorption rate is seen to be constant at the beginning of the experiment, as seen from the linearity of the graph in this region. The slope of this linear region provides the

initial absorption rate (mol CO_2/s). A general expression for the initial absorption rate (mol/(m^2 s)) is derived from this loading rate divided by the cross-sectional area of the reactor. This initial region was determined to be 20% of the time elapsed until equilibrium, and a linear fit was made to calculate the initial rate of absorption. An example of this procedure can be seen in Figure 9.

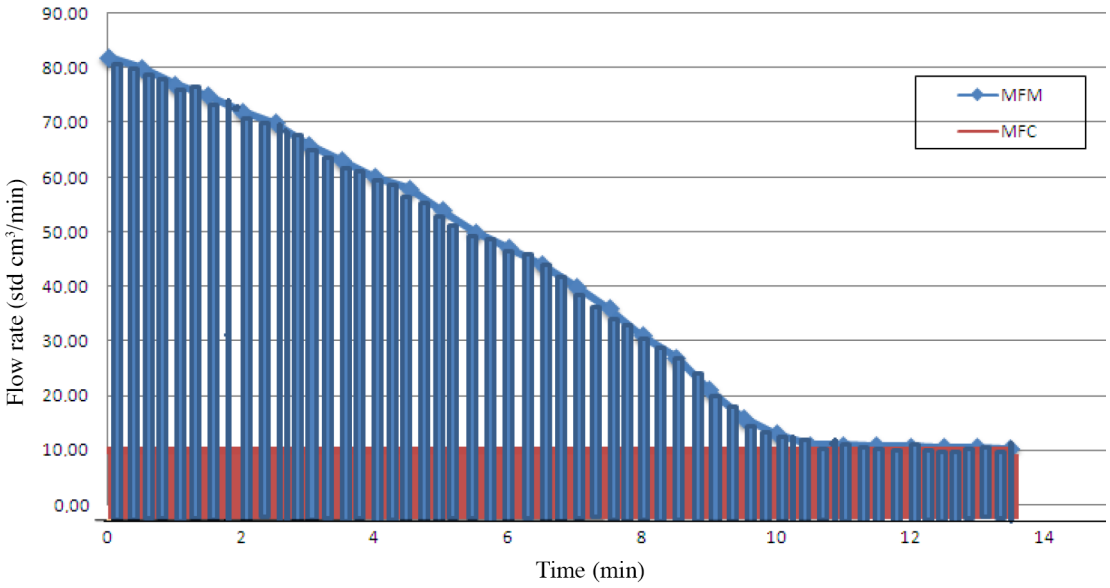

Figure 7. Fragmentation of the area between the MFM and MFC to the rectangular areas.

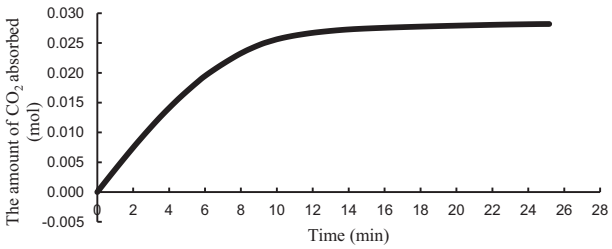

Figure 8. Typical CO_2 loading graph.

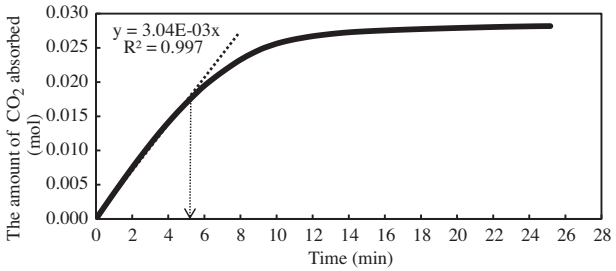

Figure 9. Calculation of slope by fitting CO_2 loading graph.

4.1.3. Stopped-flow method

Intrinsic reaction kinetics experiments were carried out to determine the rate constants of CO_2 with a solution of TMG/1-propanol by a stopped-flow apparatus (Hi-Tech Scientific, UK; Model SF-61SX2). The equipment consists of 4 main units: a sample handling unit, a conductivity detection cell, an A/D converter, and a microprocessor unit. The stopped-flow apparatus calculates the observed reaction rate constant by measuring conductivity change during the reaction. During an experimental run, CO_2 solution is placed into one syringe and the solution (TMG/1-propanol) is placed into the other syringe. Equal volumes of 2 mixtures are mixed instantaneously at the mixing chamber and the flow is stopped for the reaction to occur. The change in conductivity with time is measured by the conductivity detection unit. Then the equipment software (Kinetic Studio) calculates the observed pseudo-first-order-rate constant (k_o) based on least squares regression. To

satisfy the pseudo-first-order condition, the molar ratio of TMG to CO_2 was kept greater than 10 for any run. Each experimental set is repeated at least 10 times to achieve consistent k_o values at specified conditions. A typical graphical output is shown in Figure 10 for 5.0 wt % TMG in the 1-propanol system at 298 K; similar outputs were obtained for other reaction systems studied.

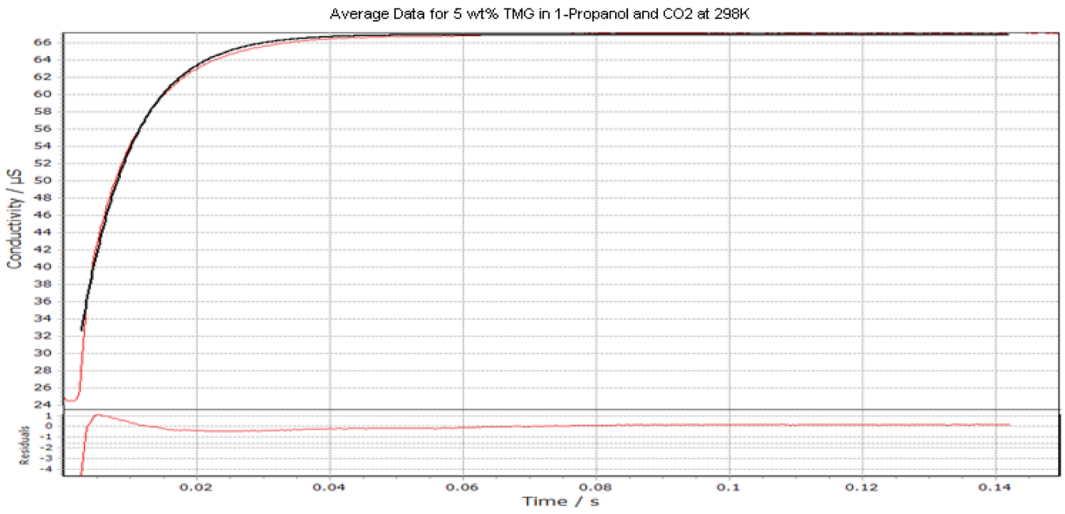

Figure 10. Typical combined graph for the 5 wt % TMG/1-propanol system at 298 K.

5. Conclusions

In this work, the reaction kinetics and absorption performance of TMG and carbon dioxide in 1-propanol medium were studied. Measurements showed that this CO_2BOL system has the ability to absorb CO_2 at a 1:1 molar ratio, which is a significant advantage in terms of CO_2 loading capacity. In addition, CO_2BOLs were recycled 5 times by desorption under a N_2 blanket at 343 K without any considerable loss of capture capacity. Finally, FTIR analyses confirmed complete reversibility of the reaction between CO_2 and TMG/1-propanol solution. These results indicate that the TMG/1-propanol/CO_2 system is a convenient switchable solvent where sudden change of medium from nonionic to ionic liquid is desired.

Kinetic experiments were performed by stopped-flow technique in the temperature range of 288–308 K over a concentration range of 0.350–1.430 kmol/m^3. The results were in agreement with a single-step termolecular reaction mechanism. For this CO_2BOL system, the reaction rate was found to depend on superbase (TMG) concentration and the temperature. A reaction rate constant of 199.30 m^3 $kmol^{-1}$ s^{-1} with a reaction order of 0.992 was obtained at 298 K for the TMG/1-propanol system. The observed rate constants obtained in this work are lower than those of the other carbon dioxide capture agents such as commercial amines.[36,39] However, this can be enhanced by addition of small quantities of promoters such as piperazine and its derivatives.

The activation energies for the TMG/1-propanol system were 5.19 kJ/mol at 2.5 wt % TMG and 5.26 kJ/mol at 5.0 wt % TMG, which seemed consistent and lower than those of various CO_2BOLs. This may offer lower regeneration heat over conventional amines, but further research is needed regarding the heats of absorption and desorption. In such a case, important energy savings during the stripping of CO_2BOLs may be possible. Therefore, further work should be conducted to provide a comprehensive insight into the performance of CO_2BOLs as carbon capture agents.

Acknowledgment

This work has been supported by the Scientific and Technological Research Council of Turkey through research grants 106M034, 107M594, and 112M446. The authors gratefully acknowledge this support.

References

1. Heldebrant, D. J.; Yonker, C. R.; Jessop, P. G.; Phan, L. In *Greenhouse Gas Control Techn. 9,* Proceedings of the 9th International Conference on Greenhouse Gas Control Technologies (GHGT-9), Washington DC, USA, 16–20 November 2008; Gale, J.; Herzog, H.; Braitsch, J., Eds; Elsevier: Amsterdam, 2009, pp. 1187–1195.
2. Camper, D.; Bara, E. J.; Gin, D. L.; Noble, R. D. *Ind. Eng. Chem. Res.* **2008**, *47*, 8496–8498.
3. Bougie, F.; Iliuta, M. C. *Chem. Eng. Sci.* **2010**, *65*, 4746–4750.
4. Gordesli, F. P.; Ume, C. S.; Alper, E. *Int. J. Chem. Kinet.* **2013**, *45*, 566–573.
5. Ume, C. S.; Ozturk, M. C.; Alper, E. *Chem. Eng. Technol.* **2012**, *35*, 464–468.
6. Ume, C. S.; Alper, E. *Turk. J. Chem.* **2012**, *36*, 427–435.
7. Heldebrant, D. J.; Yonker, C. R.; Jessop, P. G.; Phan, L. *Chem- Eur. J.* **2009**, *15*, 7619–7627.
8. Heldebrant, D. J.; Koech, P. K.; Yonker, C. R. *Energ. Environ. Sci.* **2010**, *3*, 111–113.
9. Heldebrant, D. J.; Koech, P. K.; Trisha, M.; Ang, C.; Liang, C.; Rainbolt, J.; Yonker, C. R.; Jessop, P. G. *Green Chem.* **2010**, *12*, 713–721.
10. Kim, M.; Park J. W. *Chem. Commun.* **2010**, *46*, 2507–2509.
11. Heldebrant, D. J.; Koech, P. K.; Rainbolt, J. E.; Zheng, F.; Smurthwaite, T.; Freeman, C. J.; Oss, M.; Leito, I. *Chem. Eng. J.* **2011**, *171*, 794–800.
12. Jessop, P. G.; Mercer, S. M.; Heldebrant, D. J. *Energ. Environ. Sci.* **2012**, *5*, 7240–7253.
13. Heldebrant, D. J.; Yonker, C. R.; Jessop, P. G.; Phan, L. *Energ. Environ. Sci.* **2008**, *1*, 487–493.
14. Kraft, A., Peters, L.; Johann, S.; Reichert, A.; Osterad, F.; Fröhlich, R. *Mat. Sci. Eng. C-Bio. S.* **2001**, *18*, 9–13.
15. Galezowski, W.; Jarczewski, A.; Stanczyk, M.; Brzezinski, B.; Bartil, F.; Zundel, G. *J. Chem. Soc., Faraday T.* **1997**, *93*, 2515–2518.
16. Heldebrant, D. J.; Jessop, P. G.; Thomas, C. A.; Eckert, C. A.; Liotta, C. L. *J. Org. Chem.* **2005**, *70*, 5335–5338.
17. Sharma, M. M.; Danckwerts, P. V.; *T. Faraday Soc.* **1963**, *59*, 386–395.
18. Yamada, T.; Lukac, P. J.; Yu, T.; Weiss, R. G. *Chem. Mater.* **2007**, *19*, 4761–4768.
19. Hart, R.; Pollet, P.; Hahne, D.; John, E.; Lıopis-Mestre, V., Blasucci, V.; Huttenhower, H.; Leitner, W.; Eckert, C. A.; Liotta, C. L. *Tetrahedron* **2010**, *66*, 1082–1090.
20. Phan, L.; Chiu, D.; Heldebrant, D. J.; Huttenhower, H.; John, E.; Li, X.; Pollet, P.; Wang, R.; Eckert, C. A.; Liotta, C. L.; et al. *Ind. Eng. Chem. Res.* **2008**, *47*, 539–545.
21. Yu, T.; Yamada, T.; Gaviola, G. C.; Weiss, R. G. *Chem. Mater.* **2008**, *20*, 5337–5344.
22. Liu, Y.; Jessop, P. G.; Cunningham, M.; Eckert, C. A.; Liotta, C. L. *Science* **2006**, *313*, 958–960.
23. Jessop, P. G.; Heldebrant, D. J.; Li, X.; Eckert, C. A.; Liotta, C. L. *Nature* **2005**, *436*, 1102–1102.
24. Wang, C. M.; Mahurin, S. M.; Luo, H.; Baker, G. A.; Li, H.; Dai, S. *Green Chem.* **2010**, *12*, 870–874.
25. Privalova, E.; Nurmi, M.; Maranon, M. S.; Murzina, E. V.; Maki-Arvela, P.; Eranen, K.; Murzin, D. Y. *Sep. Purif. Technol.* **2012**, *97*, 42–50.
26. Wang, C.; Luo, H.; Luo, X.; Li, H.; Dai, S. *Green Chem.* **2010**, *12*, 2019–2013.
27. Pollet, P.; Eckert, C. A.; Liotta, C. L. *Chemical Sciences* **2011**, *2*, 609–614.
28. Barzagli, F.; Vaira, M.; Mani, F.; Peruzzini, M. *Chem. Sus. Chem.* **2012**, *5*, 1724–1731.

29. Heldebrant, D. J.; Koech, P. K.; Rainbolt, J. E.; Zheng, R. 10th International Conference on Greenhouse Gas Control Technologies, Amsterdam, the Netherlands, 19–23 September 2010; Gale, J.; Hendriks, C.; Turkenberg, W., Eds; Elsevier: Amsterdam, 2011, p. 216–223.
30. Ozturk, M. C.; Ume, C. S.; Alper, E. *Chem. Eng. Technol.* **2012**, *35*, 2093–2098.
31. Caplow, M. *J. Am. Chem. Soc.* **1968**, *90*, 6795–6803.
32. Danckwerts, P. V. *Chem. Eng. Sci.* **1979**, *34*, 443–446.
33. Ume, C. S.; Alper, E.; Gordesli, F. P. *Int. J. Chem. Kinet.* **2013**, *45*, 161–167.
34. Davis, R. A.; Sandall, O. C. *Chem. Eng. Sci.* **1993**, *48*, 3187–3193.
35. Crooks, J. E.; Donnellan, J. P. J. *Chem. Soc. Perk. T.* **1989**, *2*, 331–333.
36. Alper, E. *Chem. Eng. J. Bioch. Eng.* **1990**, *44*, 107–111.
37. da Silva, E. F.; Svendsen, H. F. *Ind. Eng. Chem. Res.* **2004**, *43*, 3413–3418.
38. Arslan, B. Master of Science Thesis, Faculty of Engineering, Hacettepe University, Turkey, 2012.
39. Alper, E. *Ind. Eng. Chem. Res.* **1990**, *29*, 1725–1728.
40. Ozturk, M. C.; Yuksel Orhan O.; Alper, E. *Int. J. Greenh. Gas Con.* **2014**, *26*, 76–82. (http://dx.doi.org/10.1016/j.ijggc.2014.04.023).